# POWER REFLECTIVITY FROM SURFACE FILMS

M.W. EVANS

*Department of Physics, University College of Swansea, Swansea SA2 8PP, UK*

Received 2 June 1986; in final form 22 July 1986

The admittance technique is used to solve Maxwell's equations for an inhomogenous system consisting of a surface liquid film of low-absorbing (insulating) material on a metallic aluminium substrate. The power reflectivity spectrum in $\sigma$ and $\pi$ polarisation is easily discernible and is amplified to full scale for most angles of incidence. The reflectivity spectrum is very sensitive to the thickness of the liquid film and to the angle of incidence. This provides scope for using this technique to detect thin films of polymer material on metal substrates, oxide films, interfaces and so on.

## 1. Introduction

In recent work [1–3] we have introduced the concept of variable-angle reflectivity from inhomogenous media where Maxwell's equations for the system were solved using an admittance function as introduced by Jacobsson [4] and developed by Hild [5–7]. In this paper we develop the method for a surface layer which consists of a low-absorbing medium deposited on a pure aluminium substrate. Maxwell's equations for this system are solved for incident radiation at various angles of incidence and the power reflection coefficients are determined theoretically as a function of the wave number. The results show that the reflected radiation is sensitive to the angle of incidence and also to the depth of surface material deposited on the substrate. Even when the static and infinite-frequency permittivity are separated by only about 0.5, the reflectivity spectrum is amplified to full scale by the presence of the aluminium substrate. This produces an interesting new method of investigating the spectrum of a non-dipolar material on a highly reflecting substrate. It can be used to measure the power absorption coefficient of material in thin-film form which can otherwise only be studied under conditions suitable for absorption coefficient measurement, using a thick specimen several centimetres in diameter. Thus non-dipolar monolayers could be studied in this way. New applications of this method could be in the study of, for example, material interfaces and oxide surface films on reflective metal substrates.

0009-2614/86/$ 03.50 

## 2. Theoretical methods

The electric and magnetic field vectors $\boldsymbol{E}$ and $\boldsymbol{H}$ of angular frequency $\omega$ obey the following differential equations in an inhomogenous medium of relative permittivity $\hat{\epsilon}$ (usually a complex function) and a relative permeability of $\mu = 1$:

$$\Delta \boldsymbol{E} + \frac{\omega^2}{c^2}\hat{\epsilon}\boldsymbol{E} - \text{grad div}\,\boldsymbol{E} = \boldsymbol{0}\,, \tag{1}$$

$$\Delta \boldsymbol{H} + \frac{\omega^2}{c^2}\hat{\epsilon}\boldsymbol{H} + \frac{1}{\epsilon}(\text{grad}\,\hat{\epsilon} \times \text{rot}\,\boldsymbol{H}) = \boldsymbol{0}\,. \tag{2}$$

It is assumed that the system is infinite in the $z$ and $y$ directions and inhomogenous only along the $z$ axis:

$$\hat{\epsilon} = \hat{\epsilon}(z)\,. \tag{3}$$

The interfaces in the system are parallel to the $xy$ plane and the surface layer is on a homogenous aluminium substrate of infinite thickness. In this system the dependence of the field vector on $z$ will be treated separately for $\sigma$ and $\pi$ polarisation. In $\pi$ polarisation the electric field is parallel to the plane of incidence, whilst for $\sigma$ polarisation it is perpendicular. $\sigma$ polarisation corresponds to the transverse electric (TE) mode with $\boldsymbol{E}$ in the $y$ direction, and $\pi$ polarisation to the transverse magnetic (TM) mode with $\boldsymbol{H}$ in the $y$ direction. The transverse field components $E_y$ and $H_y$ then obey the following differential equations:

$$\frac{\partial^2 E_y}{\partial z^2} + \frac{\omega^2}{c^2} (\hat{\epsilon} - \sin^2\phi_0) E_y = 0 , \quad (4)$$

$$\frac{\partial}{\partial z}\left(\frac{1}{\hat{\epsilon}} \frac{\partial H_y}{\partial z}\right) + \frac{\omega^2}{c^2}\left(1 - \frac{\sin^2\phi_0}{\hat{\epsilon}}\right) H_y = 0 . \quad (5)$$

If the admittance function is defined as

$$\hat{j}(z) = -\left(\frac{\mu_0}{\epsilon_0}\right)^{1/2} \frac{H_t(z)}{E_t(z)} \quad (6)$$

then, according to the boundary conditions of Maxwell's equations, $H_t$ and $E_t$ are continuous transverse components and so $\hat{j}(z)$ is a continuous function of $z$, unless $E_t = 0$ when the admittance function becomes infinite. The interaction of electromagnetic radiation with the inhomogenous system can then be described by the following differential equations in the admittance function:

$$\frac{d\hat{j}_{TE}}{dz} = -\frac{i\omega}{c} (\hat{\epsilon} - \sin^2\phi_0 - \hat{j}_{TE}^2) , \quad (7)$$

$$\frac{d\hat{j}_{TM}}{dz} = -\frac{i\omega}{c}\left[\left(1 - \frac{\sin^2\phi_0}{\hat{\epsilon}}\right) \hat{j}_{TM}^2 - \hat{\epsilon}\right] . \quad (8)$$

These equations can be solved using the method of Hild and Grofscik [6]; this method is described fully for epitaxial semiconductors in a recent paper by Hild and Evans [2]. Particularly significant effects were found in epitaxials near the Brewster angle and it is shown in this Letter that this is also the case for non-dipolar absorbing liquid films on an aluminium substrate.

## 3. Optical coefficients for the aluminium substrate [8]

The optical properties of metallic aluminium have been investigated thoroughly from the far infrared to the ultraviolet, and it can be estimated that the permittivity of metallic aluminium up to about 200 $cm^{-1}$ is $\approx 1.5$ and approximately constant and the dielectric loss $\approx 320000$ and approximately constant [8]. Therefore, in the calculations for this paper it was convenient to investigate the reflectivity from the inhomogenous system represented by a highly reflecting or absorbing substrate (pure metallic aluminium) and a thin film of material with the dielectric properties of an insulator deposited on the surface of the aluminium. This is a type of system often encountered in practice, for example when a metal surface becomes covered with a surface layer of oxide. By looking at the $\pi$ polarisation of the surface layer at low angles [3] it is possible to observe the reflectivity spectrum of the surface layer.

## 4. Illustrative results

The dielectric properties of the surface layer are illustrated in fig. 1 for static permittivities of 10 and 4 and an infinite-frequency permittivity of 3.5. The frequency dependence of the dielectric loss and permittivity is calculated from three-variable Mori theory as described in the literature [9]. This type of surface property is used purely for illustrative purposes and in general any type of absorption spectrum could be incorporated into the program and used to generate a reflectivity curve for the system.

Fig. 2 illustrates how the low-amplitude simple loss curve of fig. 1 is amplified to full scale by depositing thin layers of the low absorber on the metallic aluminium substrate. At normal incidence, the reflectivity in both polarisations is identical, and is illustrated for $\epsilon_0 = 10$ and a surface thickness of $10^{-2}$ cm in fig. 2a. As the angle of incidence deviates from the normal, the pattern of reflectivity changes, and the frequency

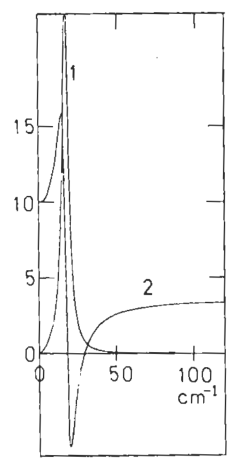


Fig. 1. Dielectric loss (1) and permittivity (2) for $\epsilon_0 = 10.0$ and $\epsilon_\infty = 3.5$. These curves are used to generate the reflectivity of fig. 2.

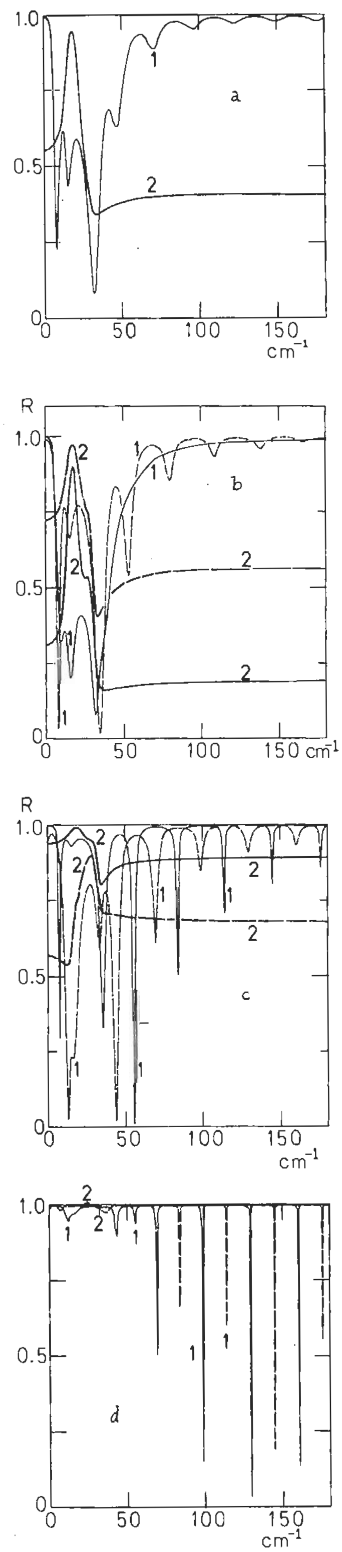


dependence of the $\pi$ and $\sigma$ reflectivity changes. Fig. 2b illustrates this for an incidence angle of 60° and fig. 2c for 85°. It can be seen that as the Brewster angle of 89.8987° is approached, the interference fringes become sharper and the lower-frequency features weaken in amplitude. Therefore, by sweeping through the angles, a series of power reflectivity fingerprints of the original absorption spectrum is generated. The set of fingerprints is acutely sensitive to the depth of a surface liquid film, and small changes in thickness of this film result in large changes in the power reflection profile. This is useful for applications, and the first results using this technique have already been obtained [10].

### 4.1. *Reflectivity from monolayers*

By a suitable choice of conditions it is possible to detect the $\pi$-polarisation reflectivity spectrum from a surface layer of 1 Å thickness. Using the parameters $\epsilon_0 = 70.0$, $\epsilon_\infty = 3.5$, and the three variables of the Mori theory [9] $\phi_0(0) = 1.0 \times 10^{25}\ s^{-2} = \phi_1(0)$; $\gamma = 1.0 \times 10^{13}\ s^{-1}$, fig. 3 illustrates the $\pi$-polarisation reflectivity at angles above and below the Brewster angle $\phi_B$ = 89.8987°. The $\sigma$-polarisation reflectivity for this thickness of surface layer is unity for all incidence angles, but the feature of interest in fig. 3 is associated with the frequency at which the permittivity changes sign (from negative to positive). The shape of this feature under all conditions is strongly dependent on polarisation, angle of incidence, and thickness of the surface layer. This makes it useful for applications to low-dimensional materials of all kinds in the context of infrared reflectivity at variable incidence angle.

As the incidence angle is increased from 89.50° (curve (1) of fig. 3) to very near the Brewster angle at 89.90° (curve (4)) the background level of $\pi$-polarisation reflectivity falls and reaches a minimum at the Brewster angle of 89.8987° determined by the proper-

Fig. 2. Power reflectivity for $\epsilon_0 = 10.0$ for various angles of incidence: (a) Normal incidence ($\phi = 0$). (1) 0.01 cm of liquid on Al substrate. (2) Reflectivity from the surface of the homogenous liquid, with the Al substrate removed (see appendix). The difference between curves (1) and (2) illustrates the effect of the Al substrate. (b) $\phi = 60°$, – – – $R_\sigma$; ——— $R_\pi$. (c) $\phi = 85°$, – – – $R_\pi$; ——— $R_\sigma$. (d) $\phi$ = 89.8987°, ——— $R_\sigma$; – – – $R_\pi$. Curves (2) of fig. 2 illustrate the reflectivity in $\sigma$ and $\pi$ polarisation from the pure liquid. Curves (2) are calculated from the analytical equations of the appendix. This illustrates the effect of the metal substrate on the reflectivity from the surface liquid film.

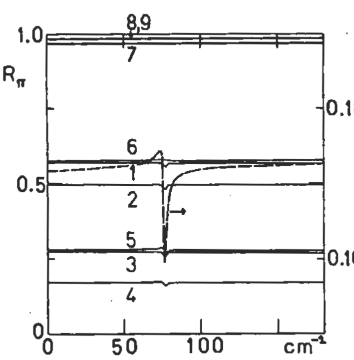


Fig. 3. $\pi$-polarisation power reflection coefficient from a surface liquid film of 1 Å thickness for $\epsilon_0 = 70$, $\epsilon_\infty = 3.5$ and the Mori parameters of the text. The film is deposited on pure metallic aluminium. Note that the high-frequency 76 cm$^{-1}$ feature is visible in fig. 3 as a blip on the solid curves (1)–(6), which are for incidence angles of, respectively, 89.500°, 89.700°, 89.800°, 89.900°, 89.950°, and 89.980°. The dashed curve (right-hand scale) is the reflectivity at the Brewster angle itself (89.8987°). Curves (7)–(9) of this figure are for $R_\pi$ from a 1 Å film deposited on a substrate with zero dielectric loss and permittivity 1.5. Note that the 76 cm$^{-1}$ feature has disappeared in curves (7)–(9) which are for incidence angles of 89.8°, 89.8987° and 89.98°.

ties of pure metallic aluminium up to about 200 cm$^{-1}$. Superimposed on the background levels in curves (1) to (4) is the residual high-frequency feature at 76 cm$^{-1}$. This small inverted peak is enlarged for clarity in the dashed curve (right-hand ordinate of fig. 3) which is drawn at the Brewster angle itself. The minimum background level of 0.173 occurs at this angle and is determined by the substrate. On the other hand the 76 cm$^{-1}$ inverted peak is a property of the surface film, whose dielectric loss and permittivity are those of fig. 1. After sweeping through the Brewster angle (curves (5) and (6) of fig. 3) the background level rises rapidly to unity for all $\bar{\nu}$ at $\phi = 90.0000°$. If the surface layer is being analyzed, the feature at 76 cm$^{-1}$ should be concentrated on; if we are interested in the substrate, we note the fall and rise of the background level as we sweep through the Brewster angle in $\pi$ polarisation. (In $\sigma$ polarisation the 76 cm$^{-1}$ feature dis-

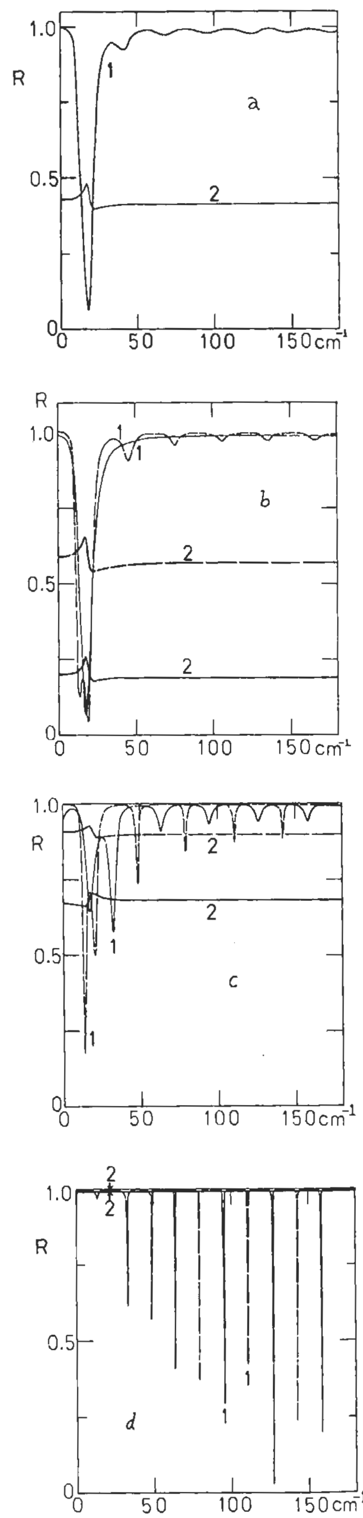


Fig. 4. As for fig. 2 using a static permittivity reduced to 4.0. (a) Normal incidence ($\phi = 0$). Curves (1) with metal, curves (2) without metal. (b) $\phi = 60°$; – – – $R_\sigma$; ——— $R_\pi$, curves as for (a). (c) As for (b) $\phi = 85°$. (d) As for (b) $\phi = 89.8987°$.

appears and the power-reflectivity coefficient remains near unity for all $\bar{\nu}$ and $\phi$.) The rise and fall in $\pi$ polarisation of the background level show that the $\pi$ reflectivity from metallic aluminium is a minimum at the Brewster angle. This feature leads to an experimental method for measuring the optical properties of a metal in the far infrared and microwave regions.

A surface film *of only 1* Å in thickness is detectable as shown in fig. 3 (and also at lower incidence angles). This is made possible by using a near-perfect reflector as substrate. If we replace the Al substrate with one whose static (assumed constant) dielectric permittivity is 1.5 and whose dielectric loss is zero (in contrast to 320000 for Al) the high-frequency 76 $cm^{-1}$ feature vanishes completely and we are left with curves (7)–(9) of fig. 3 at the incidence angles commensurate with those of curves (1)–(6) for the Al substrate. This amplification of the high-frequency feature emerges naturally from Maxwell's equations. The amplification is at its most effective near the Brewster angle, which for a near-perfect reflector will be arc minutes above the parallel. This again seems to be a new principle. In simple physical terms the phenomenon is explained by the fact that a ray of light travelling nearly parallel to a mirror-like substrate will have the greatest chance of detecting an extremely thin film deposited on the surface of the mirror.

### 4.2. *Very-low-reflecting surface layer*

Fig. 4 shows the reflectivity spectra for a zero-frequency permittivity in the surface layer of 4.0 and an infinite-frequency permittivity of 3.5. Such a surface layer would correspond to a low absorber, e.g. a non-dipolar liquid or a polymer. Consequently the method introduced here would be of use in investigating the properties of ultra-thin polymer films on metals. In fig. 4a the incidence angle is zero (normal incidence) and it can be seen that the original absorption spectrum is amplified to full scale and could easily be measured accurately in the laboratory. As the angle of incidence is varied, the $\pi$ and $\sigma$ components of the power reflectivity separate out (both are to full scale), providing a useful set of fingerprints for experimental investigation of the inhomogenous film/metal system. As in fig. 2, as the angle increases, the interference fringes sharpen and the lower-frequency feature becomes less pronounced and shifted considerably in frequency dependence. This gives scope for identification purposes if the present technique is used for chemical analysis and identification of unknown surface materials. Again, the spectrum is sensitive to small changes in the thickness of the surface film, and this is useful for analysis.

In order to implement the reflectivity method at near-parallel glancing angles it is advantageous to use radiation in the near infrared, visible or ultraviolet, where the wavelength is fairly short and the optical collimation of the beam can be made very precise. It is an advantage at very low angles to use beams which are as narrow as possible, so that as much of the beam as possible is reflected from samples of practical dimensions into the detector. Given these considerations the amplification effect of the metal substrate illustrated in fig. 4 will allow the detection of thin layers of low-absorbing material on reflecting substrates.

## Acknowledgement

The University of Wales is thanked for financial support, and Dr. E. Hild for suggesting this analysis. Professor A.D. Buckingham is acknowledged for several suggestions, incorporated in the manuscript.

## Appendix: power reflection from the homogenous liquid

It is of interest to compare the reflectivity from the inhomogenous system represented by the surface liquid/metal substrate with the power reflectivity from the liquid alone. This will reveal the effect on the spectrum of the metal substrate.

It is possible to obtain the power reflection coefficients from the homogenous liquid system analytically from Snell's law, the Fresnel formulae and Maxwell's equations. The complete set of equations used for the relevant curves (2) in figs. 2 and 4 are given here, starting from the dielectric loss

$$\epsilon''(\omega) = \frac{(\epsilon_0 - \epsilon_\infty)\,\omega\gamma\phi_0(0)\,\phi_1(0)}{\gamma^2[\phi_0(0) - \omega^2]^2 + \omega^2\{\omega^2 - [\phi_0(0) + \phi_1(0)]\}^2} \tag{A1}$$

and permittivity

$$\epsilon'(\omega) = \epsilon_0 - (\epsilon_0 - \epsilon_\infty)\frac{\omega^2\{\gamma^2[\omega^2 - \phi_0(0)] + [\omega^2 - \phi_1(0)][\omega^2 - (\phi_0(0) + \phi_1(0))]\}}{\gamma^2[\phi_0(0) - \omega^2]^2 + \omega^2\{\omega^2 - [\phi_0(0) + \phi_1(0)]\}^2} \tag{A2}$$

from the Mori three-variable theory [9]. Here $\gamma$, $\phi_0(0)$ and $\phi_1(0)$ are the three coefficients of this formula, defined in terms of molecular parameters [9]. For the illustrations in figs. 2 and 4 we used the values in the text.

Maxwell's equations are used with the usual relation between the complex permittivity and the complex refractive index:

$$(\epsilon' - \mathrm{i}\epsilon'')^{1/2} = n(1 - \mathrm{i}\kappa)\,. \tag{A3}$$

The reflective power is then the ratio of the radiative energy reflected from the liquid surface to that incident at any wave number. It is dependent on the angle of incidence and on the state of polarisation. The direction of vibration is with respect to the plane of incidence with the liquid surface, and the component of the radiation vibrating parallel to this plane is the $\pi$ component, that perpendicular the $\sigma$. The power reflection coefficient (or reflective power) for each component is given as a function of the angle of incidence $\phi$ and the angle of refraction $\chi$ by the Fresnel formulae

$$R_\sigma = \frac{\sin^2(\phi - \chi)}{\sin^2(\phi + \chi)}, \qquad R_\pi = \frac{\tan^2(\phi - \chi)}{\tan^2(\phi + \chi)}, \tag{A4}$$

the angles being related by Snell's law:

$$\sin\phi = n'\sin\chi\,, \tag{A5}$$

where $n'$ is the frequency-dependent refractive index of the liquid. If at a given wave number the liquid absorbs, then $n'$ is complex:

$$n' = n(1 - \mathrm{i}\kappa)\,,$$

where

$$n = \{\tfrac{1}{2}[(\epsilon'^2 + \epsilon''^2)^{1/2} + \epsilon']\}^{1/2}, \qquad \kappa = \epsilon''/2n\,. \tag{A6}$$

This implies that the angle of refraction is complex:

$$n'\cos\chi = (n'^2 - \sin^2\phi)^{1/2} \equiv a - \mathrm{i}b\,. \tag{A7}$$

It follows that:

$$R_\sigma = \frac{a^2 + b^2 - 2a\cos\phi + \cos^2\phi}{a^2 + b^2 + 2a\cos\phi + \cos^2\phi}, \tag{A8}$$

$$R_\pi = R_\sigma\left(\frac{a^2 + b^2 - 2a\sin\phi\tan\phi + \sin^2\phi\tan^2\phi}{a^2 + b^2 + 2a\sin\phi\tan\phi + \sin^2\phi\tan^2\phi}\right), \tag{A9}$$

where

$$a = \frac{1}{2}\left(\frac{x_1 + x_2}{2}\right)^{1/2}, \tag{A10}$$

$$a^2 + b^2 = \frac{x_1 + x_2}{2} + \frac{2n^4\kappa^2}{x_1 + x_2}, \tag{A11}$$

with

$$x_1 = n^2(1 - \kappa^2) - \sin^2\phi\,, \qquad x_2 = (x_1^2 + 4n^4\kappa^2)^{1/2}\,. \tag{A12}$$

These relations link the power reflection coefficients in $\sigma$ and $\pi$ polarisation with the dielectric loss and permittivity of the homogenous liquid [1].

*Note that in inhomogenous media, those equations are not applicable* and the numerical admittance method of the text must be used [2].

## References


[1] M.W. Evans, J. Chem. Soc. Faraday Trans. II 76 (1980) 1147.

[2] E. Hild and M.W. Evans, J. Appl. Phys. 59 (1986) 1147.

[3] E. Hild, M.W. Evans and G.J. Evans, J. Chem. Soc. Faraday Trans. II, to be published.

[4] R. Jacobsson, Light reflection from films of continuously varying refractive index, in: Progress in optics, Vol. 5, ed. E. Wolf (North-Holland, Amsterdam, 1965).

[5] E. Hild, Doctoral Dissertation, University of Budapest, Hungary.

[6] E. Hild and A. Grofscik, Infrared Physics 18 (1978) 23.

[7] E. Hild, A. Grofscik and A. Rac, Techn. Tungs. Mitteilung 37 (1978) 1561.

[8] E. Shiles, T. Sasaki, M. Inokuti and D.Y. Smith, Phys. Rev. B22 (1980) 1612.

[9] M.W. Evans, G.J. Evans, W.T. Coffey and P. Grigolini, Molecular dynamics (Wiley–Interscience, New York, 1982).

[10] E. Hild, private communication.